Optimizing Simulations of Hydrogen Production from Methane using Factorial Design and Particle Swarm Optimization

A Thesis

Submitted to The Faculty of
The Graduate School of the

University of Minnesota

By

Brady Rau

In Partial Fulfillment of the Requirements

For the Degree Of

Master of Science in Chemical Engineering

Professor Richard A. Davis, Thesis Advisor

June 2020

TABLE OF CONTENTS

NOMENCLATURE

Abbreviations

CB	Carbon Black
CO2	Carbon Dioxide Gas
H2	Hydrogen Gas
IEA	International Energy Agency
MDEA	Methyldiethanolamine
NG	Natural Gas
NREL	National Renewable Energy Laboratory
NSRDB	National Solar Radiation Database
PSA	Pressure-Swing Adsorption
PSO	Particle Swarm Optimization
S/C	Steam-to-Carbon Ratio
SMC	Solar Methane Cracking
SMR	Steam Methane Reforming
SR	Solar Resource (W/m^2)
WGS	Water-Gas Shift

Variables

c_1	Relative Particle Acceleration Constant
c_2	Global Acceleration Constant
C_H	Cost of Heliostat ($\$/m^2$)
C_{NG}	Cost of Natural Gas ($/hr)
C_U	Cost of Utilities ($/hr)
C_W	Cost of Water ($/hr)
g_j	Global Best Condition of Population
$\dot{m}_{H_2}$	Mass Flow of Hydrogen (kg/hr)
m	Maximum Number of Iterations
η	Efficiency (%)
n	Number of Variables
p_j	Particle's Best Condition
Q	Heat Duty (W)
r_1, r_2	Random Numbers
Δt	Step Change
w	Adaptive Inertia Weighting Factor
$x_{i,j}$	Particle Location
x_j	Variable
x_j^L	Lower Bound of Variable
x_j^U	Upper Bound of Variable
$v_{i,j}$	Particle Velocity

LIST OF TABLES

LIST OF FIGURES

INTRODUCTION

Presently, ten trillion kilograms of carbon-based fossil fuels are combusted around the globe annually. However, these fuels are ever-depleting and the necessity for a replacement is fast approaching. [1] As political and environmental policies push for reducing greenhouse gas emissions to combat climate change, the need to research sustainable energy technologies has increased, and hydrogen has been emerging as a suitable energy carrier in recent years. Hydrogen has proven to have several advantages over its hydrocarbon counterparts: it burns cleanly, producing only water upon combustion; generates 39.4 kWh/kg upon combustion, which is triple the amount of other fuels; may be used in fuel cells for powering transportation; and can be stored for long periods of time, with negligible losses, for energy on demand. [2]

The International Energy Agency (IEA) developed global energy scenarios to simulate technological advances in energy, and energy supply and demand. According to their results, there will be a significant increase in hydrogen demand through the year 2050. [3] The scenarios were made in response to a call from the G8 Summit for IEA to provide guidance to international decision makers on how to act now in order to shape a future based on cleaner energy. With hydrogen being such a suitable candidate for an energy economy and these global scenarios being reported, the necessity for sustainable hydrogen production is of great significance. Amongst other studies into the future of a hydrogen economy are Pregger et. al., who studied the prospects of solar thermal hydrogen production processes and conducted a comparison on hydrogen requirements in future years. They found, under generous technological and economic assumptions, the demand

of hydrogen is to increase from its current level of 3 percent, to 8 percent in the year 2050. [3]

In today's hydrogen market, approximately 96 percent of all hydrogen produced is using steam methane reforming (SMR). [4] This technology has been well-established for decades and the U.S. produces nearly 11 million metric tons of hydrogen annually using this method. Although SMR is the mainstay in hydrogen production, it has large disadvantages relative to renewable methods in that it requires dwindling fossil fuel sources and produces a large amount of carbon emissions. Other methods of H_2 production that are in use or researched include electrolysis - which produces around four percent of the hydrogen generated today - coal gasification, biomass gasification, and photoelectrochemical decomposition of water. New methods for hydrogen production must be researched and implemented in the industry to support the combat of climate change from carbon-based fuel emissions.

THESIS PROBLEM

This thesis details the optimization of three different hydrogen production methods including SMR, solar SMR, and solar methane cracking (SMC). Each method is simulated using the chemical process simulation software, Aspen Plus [5], and the optimizations are conducted using a statistical factorial design and analysis in Minitab [6], followed by the particle swarm optimization (PSO) technique programmed into Microsoft Excel [7], using Visual Basic for Applications. The models are used to calculate the hydrogen production costs and carbon emissions of each process and the results are compared with conventional SMR to determine if solar-powered production has the potential to be competitive with conventional SMR.

Factorial Design

To test each of the hydrogen production methods, factorial experiments were designed using Minitab. A factorial design allows for multiple factors to be studied and the effects those factors have on a single response or multiple responses. To develop the design, the factors are chosen and the levels for the factors are specified. For a full factorial design, all combinations of factor levels are tested. A fractional factorial design conducts only a subset of the runs in the full factorial and is an ideal choice when the resources of the experiment are limited to reduce the number of trials. For this thesis, all experiments were conducted by simulation at a relatively low cost, hence a full factorial design and analysis was performed.

Once each of the trials of the experiments is completed, the result can be imported into Minitab for analysis. Minitab performs the statistical calculations necessary to determine the effects each factor has on each response. This is helpful when conducting an optimization, like particle swarm, because it allows for some factors to be eliminated from testing if they have a relatively small effect on the response. It also allows the factor ranges to be reduced.

Particle Swarm Optimization

The PSO method was selected for global multi-variable optimization of the three hydrogen production process simulations. This technique involves a population-based, stochastic algorithm, inspired by the collective behavior of flocks of birds or schools of fish when searching for the best food source. [8]

The PSO algorithm operates through a series of coordinated movements of population particles to locate the global optimum of an objective function. Each particle has the

properties of the optimization variables and objective function. The objective function is defined with n variables, x_j, and each variable j is given boundary constraint limits: $x^L_j < x_j < x^U_j$. The maximum number of iterations and the size of the particle populations, m, are both specified. Each particle's location is selected randomly using Latin hypercube random sampling of the search domain and then the algorithm begins a cycle to converge on the global optimum. [8]

Each particle is initialized with random coordinates, velocity, and direction in order to begin the search for the global optimum. As the particles move throughout the objective space, the particles' best-found positions are recorded, and the global best-found position is determined. Using this information, each particle's velocity vector for the next iteration of the cycle is calculated using Equation (1) that points the trajectory toward the current best position.

$$v_{i+1,j} = wv_{i,j} + r_1c_1(p_j - x_j) + r_2c_2(g_j - x_j) \quad (1)$$

where w is an adaptive inertia weighting factor with particle success feedback, $v_{i,j}$ is the particle's current velocity, c_1 and c_2 are the relative particle and global acceleration constants with values typically in the range of 1.5 to 2, and r_1 and r_2 are random numbers drawn from a uniform distribution ($0 < r < 1$). The variables, p_j and g_j, are the particle's best condition and the global best of the population of the particles, respectively. Values of $w = 0.5$ and $c_1 = c_2 = 1.5$ are used in our implementation of PSO as recommended by Hassan et. al. [9]

Each particle's next location is determined using its previous coordinates and velocity vector using Equation (2),

$$x_{i+1,j} = x_{i,j} + \Delta t v_{i+1,j} \tag{2}$$

where $x_{i,j}$ is the particle's current location and Δt is the step change.

Occasionally, a particle's movement will cause it to encroach on or surpass a variable boundary constraint. To correct this issue if it does occur, the calculated, future location is amended using the harmonic mean distances from the location to the boundary using Equation (3):

$$x_{i+1,j} = \begin{cases} x_j^L + \left(1 - \dfrac{x_{i,j} - x_j^L}{|v_{i+1,j}|}\right)\left(x_{i,j} + x_j^L\right) \; if \; x_{i+1,j} < x_j^L \\ x_j^U - \left(1 - \dfrac{x_j^U - x_{i,j}}{|v_{i+1,j}|}\right)\left(x_j^U - x_{i,j}\right) \; if \; x_{i+1,j} > x_j^U \end{cases} \tag{3}$$

The objective function values for the particles are compared against each other to determine the local and global best particles. This information is retained for future comparisons as well. When the objective function value has ceased to change, based on the given tolerance and after the given amount of cycles without change, the search ends, and the global best values are reported.

Economic Analysis

To conduct the economic analysis, a hypothetical location for the facilities was chosen. This allows for collecting reasonable values for economic information such as the costs of natural gas and water. When determining where to site the processes, the first parameter acknowledged was the solar energy available. Using information from the National Renewable Energy Laboratory (NREL) and the National Solar Radiation Database (NSRDB), shown in Figure 1, the top four candidate states were chosen: Arizona, California, Nevada, and New Mexico.

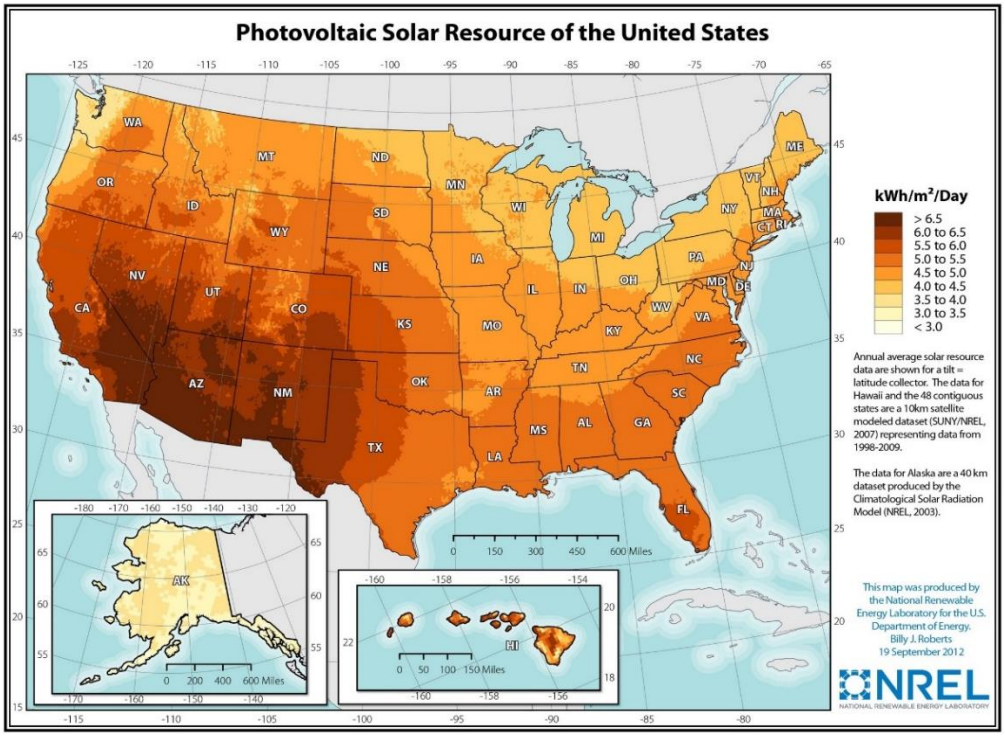

Figure 1. Map of solar resource (kWh/m^2/day) in the United States [10]

The next parameter was the cost of one of the process feeds: natural gas. The four states' natural gas prices were compared, as shown in Figure 2, and New Mexico was found to have the lowest average cost. This combination of solar irradiance and natural gas pricing led to the selection of Albuquerque, New Mexico, as the theoretical site of the facilities. Albuquerque receives approximately 6500 W/m^2 average photovoltaic solar resource (SR) daily and the industrial water price in the Albuquerque area for an 8-inch water meter is $2.25 per kGal. [10], [11]

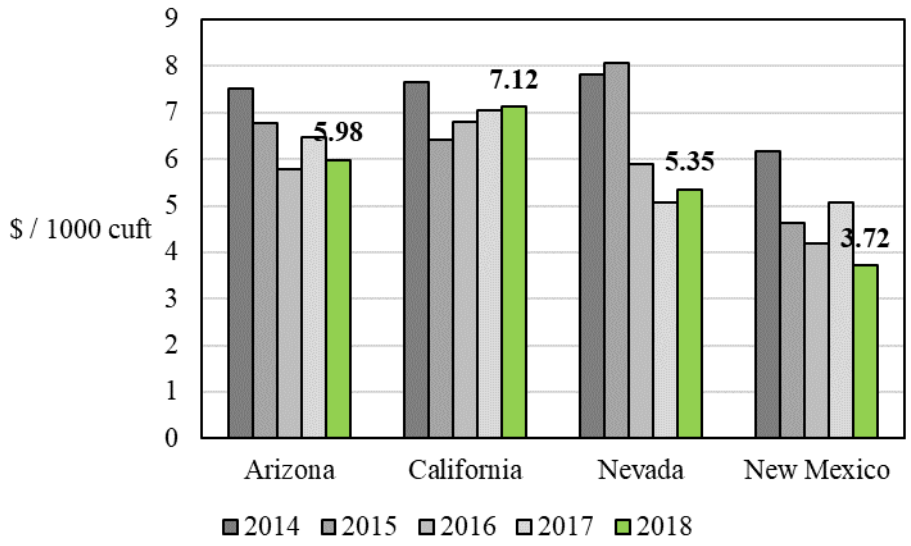

Figure 2. Natural gas pricing in prospective states [12]

Due to the different energy sources (high-temperature methane furnace for SMR and heliostats for solar SMR and SMC), the economic calculations need to be conducted differently for each energy source. For the high-temperature methane furnace, the energy cost is incorporated in the utility cost for the process and is calculated by Aspen Plus. For the heliostats, the energy cost was calculated as a cost per kilogram of hydrogen produced hourly. The amount of heat duty required for the process at optimum conditions is used to calculate the area of heliostats necessary to provide the energy. The heliostats are assumed to be 60% effective at collecting the solar energy , and as stated above, the solar resource used in the calculations is 6.5 kWh/m^2 for the city of Albuquerque, NM. By dividing this cost of heliostats by the mass of hydrogen produced by the process, the cost per kilogram of hydrogen produced hourly is calculated. Equation (4) is used for this calculation,

$$\frac{\$}{\frac{kg\ of\ H_2}{hr}} = \frac{Q}{\eta(SR)}\frac{C_H}{\dot{m}_{H_2}} \tag{4}$$

where Q is the heat duty required for the reactor (W), η is the heliostat efficiency, SR is the solar resource of the geographical location (W/m^2), C_H is the cost of heliostats per area ($/m^2), and $\dot{m}_{H_2}$ is the mass flow of hydrogen produced (kg/hr).

Amin et. al. found that hydrogen production cost for SMR follows Equation (5). [13]

$$Hydrogen\ Cost\ \left(\frac{\$}{MMBtu}\right) = 1.27 * NG\ price\ \left(\frac{\$}{MMBtu}\right) + 0.985 \qquad (5)$$

Thus given an average gross heating value for natural gas of 1,031 Btu/ft^3, the cost of the natural gas is $3.64/MMBtu. [14] The resulting hydrogen production cost is $3.61/MMBtu, or $0.49/kg. For either of the solar-powered methods to be competitive, their production cost would need to fall near this cost.

Despite this lofty goal, there has been research that shows solar-powered options have the capability to contend with their SMR counterpart. Möller et. al. conducted a comparison cost study of two hydrogen production processes: conventional SMR and solar SMR. They found that the cost of hydrogen for conventional production was $0.0456/kWh and for solar, $0.054/kWh and $0.0564/kWh with 1.5 and 3.0 S/C, respectively. [15] Parkinson et. al. conducted a study on the techno-economics of decarbonized fuels. Their research found that with innovations to reactor design and improved catalytic activity, pyrolytic hydrogen productions may be able to compete fiscally with that of SMR. [1] Graf et. al. conducted an economic study comparing thermochemical and solar energy cycles to the commercially practiced electrolysis for hydrogen production. They found, through simulation and sensitivity analysis, that hydrogen production costs ranged from 4.44-6.37 $/kg for a hybrid-sulfur cycle, 3.98-14.57 $/kg for a metal oxide-based cycle, and 2.39-7.74 $/kg for electrolysis. [16], [17] Touili et. al. conducted a technical and economical assessment on

the prospect of solar-produced hydrogen in Morocco. The group simulated the electricity and hydrogen production cost for a photovoltaic-electrolyze system at 76 sites across the country. They found that the daily annual mass of hydrogen produced ranges from 6489 – 8308 ton/km^2. The costs of electricity and hydrogen production ranged from 0.077 – 0.099 $/kWh and 4.64 – 5.79 $/kg, respectively. [2] Collectively, all this research supports the idea that the solar-powered, hydrogen-production methods can be fiscally competitive with the traditional SMR method.

PROCESS AND MODEL DESCRIPTIONS

This section describes each of the three hydrogen-producing processes in question: steam methane reforming (SMR), solar SMR, and solar methane cracking (SMC).

Steam Methane Reforming

The reaction governing SMR is shown in Equation (6). The reaction is highly endothermic and requires high temperatures in order to see any significant conversion. Typically, SMR reactions are coupled with a water-gas shift reaction (WGS) to increase both the methane conversion and the hydrogen yield while decreasing the amount of carbon monoxide emitted. The water-gas shift reaction is shown in Equation (7) and is often performed in two steps: a high temperature shift followed by a low temperature shift. By performing both steps, the yield of hydrogen is drastically increased due to the thermodynamics of the reaction. Equilibrium for this reaction favors the products at low reaction temperatures, but high temperature is required to achieve a practical reaction rate. [18] The overall reaction for the SMR process is shown in Equation (8).

$$CH_4 + H_2O \rightarrow CO + 3H_2 \quad (6)$$

$$CO + H_2O \rightarrow CO_2 + H_2 \quad (7)$$

$$CH_4 + 2H_2O \rightarrow CO_2 + 4H_2 \quad (8)$$

The natural gas feed stream characteristically has a composition that is mainly methane along with other hydrocarbons species, oxygen, nitrogen, water, etc. The typical composition of natural gas is shown in Table 1. Sulfur-containing compounds are also typically supplemented to natural gas as a safeguard in industrial settings. While this supplement is important for safety, it causes downstream issues in catalytic reactors and the catalysts are often fouled, reducing their efficiency. To avoid this issue, the sulfur components are separated from the feed stream.

Table 1. Typical natural gas composition [19]

Component	Typical Analysis (mol %)
Methane	95.0
Ethane	3.8
Propane	0.2
iso - Butane	0.02
normal - Butane	0.02
iso - Pentane	0.01
normal - Pentane	0.01
Hexanes plus	0.01
Nitrogen	0.6
Carbon Dioxide	0.3
Oxygen	0.01
Hydrogen	0.03

The steps for SMR include feed gas pre-treatment, steam reforming, water-gas shift, and gas separation. The pre-treatment step of the model is shown in Figure 3. The natural gas feed is sent to a flash separator (S1) to ensure a stream of only vapor continues in the process. While this process is defined to have a feed stream of only vapor, this step is added

to accommodate for other possible feeds. The stream is compressed (C1), and any organic sulfur compounds are hydrogenated in a zinc oxide bed (R1). This is a necessary step in pre-treatment, as any sulfur species in the stream will cause fouling of the catalysts in the following reactors. A feed water stream is fed to a steam generator (E1). The steam is then compressed to the same pressure as the natural gas (C2).

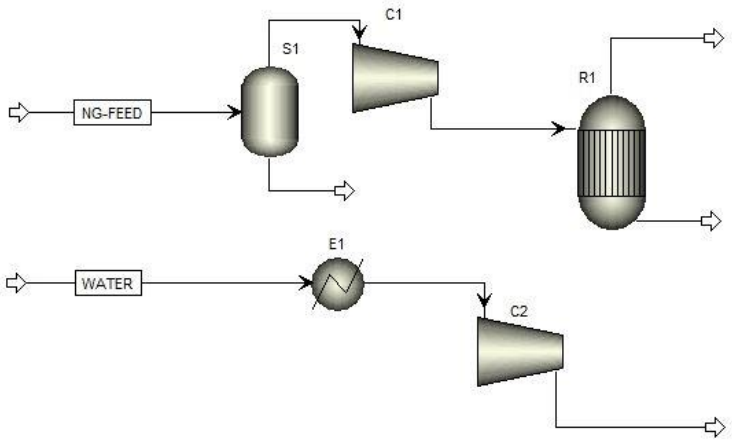

Figure 3. SMR pre-treatment phase

Following pre-treatment, the methane-rich stream is fed into a high-temperature SMR reactor to react with steam, as shown in Equation (6). Conventionally, this step is done in a gas-fired furnace at a temperature around 1123 K. The gas flows through external tubes packed with catalyst that are heated by the furnace. [20]

To increase hydrogen yield from the process, the SMR exit stream is sent to a two-stage water-gas shift reactor system. The water-gas shift reaction is shown in Equation (7). The first stage is a high-temperature shift with temperature from 623-723 K, and the second

stage is a low-temperature shift with temperature around 473 K. These stages are operated in fixed-bed catalytic reactors. [20]

The main reactors used in the SMR model are illustrated in Figure 4. The natural gas and the steam are mixed together before entering a pre-reforming reactor (R2). This reactor is used to break down any higher hydrocarbons into methane. After the pre-reforming stage, the stream is ready for the main reforming reactor (R3). The main reaction, shown in Equation (6), is highly endothermic and the energy necessary for this reactor is provided by a reformer furnace, which is not shown. Heat from the exit stream is recycled using a heat exchanger (E2) to use the heat energy in other areas of the process, such as the steam generator or the desulfurizer. The next step in the process is the water-gas shift reaction. This reaction is broken into two separate reactors for the simulation. The first reactor (R4) performs a high temperature shift, and the second reactor (R5) performs a low temperature shift. The process stream is now very rich with hydrogen; however, some separation processes are still necessary to obtain a hydrogen purity of 99.999 percent.

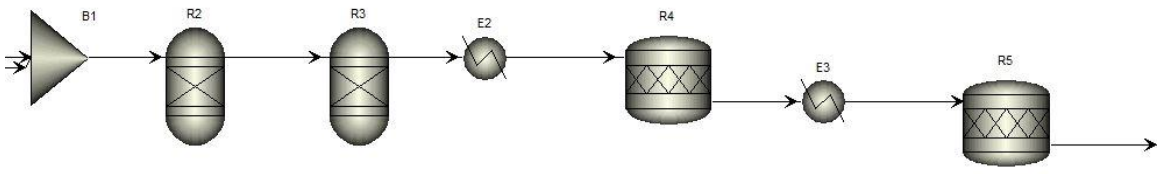

Figure 4. SMR reactors phase

Finally, following the reactors, the process streams must be separated to obtain the desired hydrogen-rich stream. The separation phase is illustrated in Figure 5. The hydrogen-rich

stream is cooled using a heat exchanger with the feedwater stream (E4). The stream is then sent to a condenser to be quenched (S2). An methyldiethanolamine (MDEA) separation process is used to absorb the excess CO_2. Typically, a removal efficiency of 90 percent is anticipated. [18] Finally, a pressure-swing adsorption (PSA) unit is used to treat the stream and produce a typical purity of 99.999 percent. This step is necessary for hydrogen used in fuel cells.

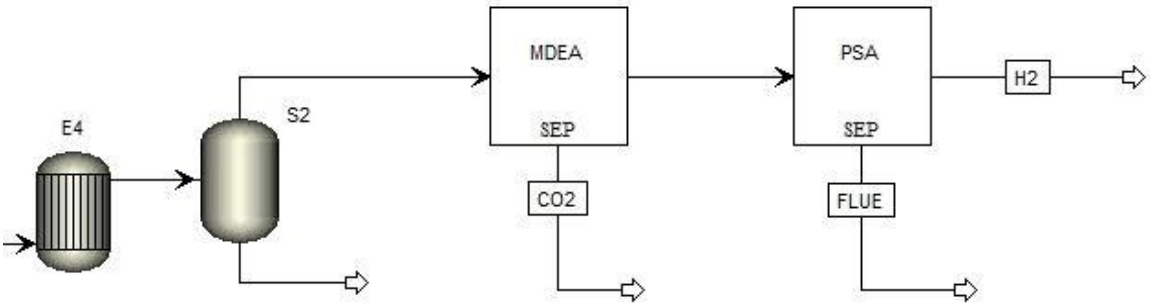

Figure 5. SMR separations phase

Solar Steam Methane Reforming

The solar SMR process follows the exact chemistry, using mainly the same equipment as the SMR process. The significant difference between these two methods is the source of the energy for the SMR reactor. While the SMR process received the energy from a high-temperature natural gas furnace, the solar version of the process uses concentrated solar energy, collected by heliostats, to heat the reactants to the necessary conversion temperature.

The SMR model was adapted to the solar energy source by removing the natural gas utility cost for the SMR reactor. Instead, the energy cost is introduced in the capital cost for a

heliostat field. The effective price of a stretched membrane heliostat is $133/m^2 and is used to calculate the associated cost, based on the energy required for the reactor. [21]

Solar Methane Cracking

Solar methane cracking (SMC) is the process of decarbonization, resulting in products of hydrogen gas and carbon black (CB). By feeding the natural gas into a high temperature reactor, the bonds between the carbon and the hydrogen groups begin to break. The decarbonization reaction is shown in Equation (8).

$$CH_4 \rightarrow C_{(s)} + 2H_2 \tag{8}$$

This reaction is an incredibly simplified version of what is most likely a complex reaction scheme. More complex reaction scheme mechanisms have been proposed to explain the production of byproducts such as acetylene, ethylene and ethane. [14], [15] In the case of the SMC, the energy required to break apart these bonds is sourced from solar energy, much like the process of the solar SMR outlined previously. The general process scheme for SMC is illustrated in Figure 6.

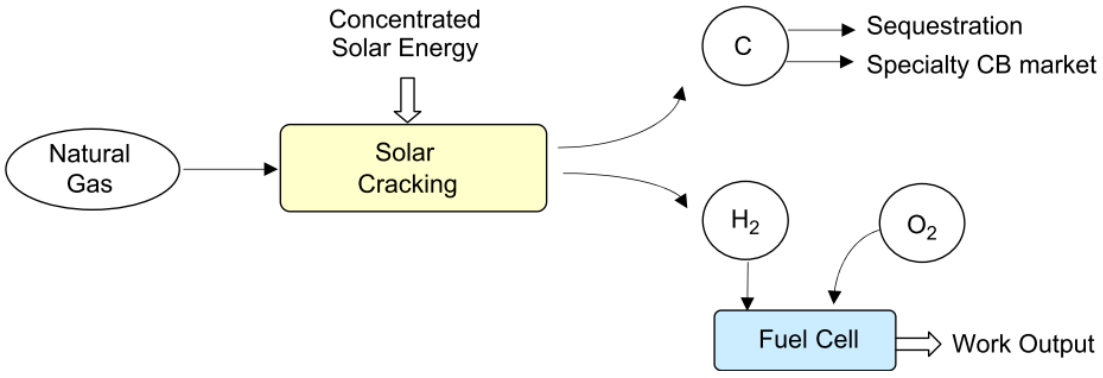

Figure 6. Basic outline of the process of solar cracking natural gas [24]

At thermodynamic equilibrium, the methane dissociation is complete for temperatures above 1500 K. [25] Complete conversion of methane was found for a methane flow rate of 0.70 kg/s at an outlet temperature of 1870 K. [26] Typically a catalyst is used in the reactor to reduce this temperature. For the purposes of this research, a Gibbs reactor is used in the simulation. By using a Gibbs reactor, the results will reflect a more perfect setting for the process. If a more perfect setting of the process is not competitive with current methods, then neither would a more realistic setting. The separation scheme in this process is quite simple, as the CB comes out as a solid and the hydrogen remains a gas. However, a PSA system is used to ensure that the hydrogen-rich stream has a purity of at least 99.999 percent, for use in fuel cells.

Although the hydrogen gas is the focused product in this case, the CB has economic value. By using this process as opposed to the conventional SMR, the carbon emissions and energy savings are positively impacted, with 14 kg of carbon dioxide being mitigated and 277 MJ per kilogram hydrogen produced. The projected costs of hydrogen depend on the price of the CB byproduct. With a CB selling price of 0.75 $/kg, the hydrogen production costs are estimated to be 15.93 $/ GJ. When the selling price increases to 0.91 $/kg, the production cost decreases to 11.38 $/GJ. [24] By incorporating the byproduct credit from CB production, Amin et. al found methane cracking can become economically favored over steam reforming. The net costs for producing 10^6 Btu of hydrogen are $5.1 and $5.9, respectively. This comes with methane cracking gaining more by-product credit for CB than the excess steam from SMR. [13]

Currently, hydrogen and CB are mainly produced via SMR and the furnace method, respectively. These two processes emit large amounts of CO_2. Estimates show that SMR produces 11.9 kg CO_2 per kg H_2 and the furnace process produces about 5.7 kg CO_2 per kg CB. By implementing solar thermal methane cracking, rather than these two previously mentioned processes, approximately 92 percent of the carbon emissions associated with the processes can be eliminated. [27]

With hydrogen demand projected to increase, much research has been conducted into improving solar methane technology. Some examples of improvements in research include catalyst implementation, improved solar energy collection, and membrane utilization.

Hirsch et. al. evaluated four routes for utilizing the power of chemical products from solar thermal decarbonization of natural gas. They have stated that the theoretical maximum closed cycle exergy efficiency, which is defined as the ratio of the Gibbs free energy change of the reaction to the solar power input, can be as high as 35 percent when using a black-body solar cavity-receiver/reactor at a temperature of 1500 K. [25]

Hu et. al. applied the density function theory to the deposition of pyrolytic carbon caused by methane pyrolysis. They recommend the reacting temperature be above 1200 K, in accordance with equilibrium. They also found that the main limiting steps of the reaction are the dehydrogenations of methane and ethylene. Their research concluded that the path of hydrogen radical attacking reactions is the best, due to its relatively low energy barrier at 1200 K of 185.7 kJ/mol. [28]

Nezzari and Gomri studied methane cracking using solar energy. The methane feed flow rate was varied, and the results showed that for the two cases of maximum solar radiation at 5 and 16 MW/m^2, the hydrogen production was in the range of 0.58 – 0.62 L/min. [29]

Rodat et. al. conducted experiments on a prototype scale solar reactor for thermal methane dissociation. The temperature range of the experiments was from 1740 to 2070 K. A theoretical 55 MW solar tower was analyzed, and production of hydrogen and CB was found to be 1.7 and 5 tons per hour, respectively. These results coincide with hydrogen production prices that are competitive with those of conventional SMR. [27]

RESULTS AND DISCUSSION

Using Minitab software, a factorial experiment was designed for each of the three methods. For SMR, the parameters of temperature and steam-to-carbon ratio were varied from 860 to 900°C and two to three, respectively. Pressure was not varied in this experiment because the thermodynamics of the governing reactions suggest that the reaction is improved with low pressure. The feed pressure for all the SMR experiment trials was set to 10 bar, to account for the pressure drops in the equipment. The first step was to design the experiment and evaluate the results of the Aspen simulation model. The factorial design table for the experiment is shown in Table 2.

Table 2. Example of the design table created by Minitab for the SMR experiment

Run	T	S/C
1	860	2.0
2	860	2.2
3	860	2.4
4	860	2.6
5	860	2.8
6	860	3.0
7	864	2.0
8	864	2.2
9	864	2.4
10	864	2.6

The experimental runs were imported into the Aspen Plus simulation using Microsoft Excel. To do this, a scenario table was made using the Aspen Simulation Workbook add-on in Excel. The scenario table allows for the simulation of many cases to be run quickly, and this is perfect for implementing the Minitab experiment.

		Input		Output				
Scenario	Active	SMR T.TEMP	Water Feed.MIXED	Water Cost.STCOST	Utility Cost.TOTUTCOST	NG Cost.STCOST	H2 Out.H2	Status
		C	kmol/hr	$/sec	$/sec	$/sec	kg/hr	
Case 1	*	860	2	1.61E-05	8.61E-04	2.59E-06	7.08	Results Available
Case 2	*	860	2.2	1.77E-05	9.38E-04	2.59E-06	7.15	Results Available
Case 3	*	860	2.4	1.93E-05	9.77E-04	2.59E-06	7.20	Results Available

Figure 7. Example of the scenario table used in Excel

In Figure 8, the data shows that the mass of hydrogen increases as both the temperature and the steam-to-carbon ratio increase. This follows the expected result, as increasing the temperature causes the highly endothermic reaction to converge on its equilibrium temperature. Increasing the S/C also allows for a higher yield of hydrogen as increasing

the amount of water means hydrogen becomes the limiting reactant. Although these factors improve the yield of hydrogen, the focus of this research is to determine the optimum conditions to produce the most hydrogen per dollar of production cost. The mass appears to converge on an asymptote near 7.38 kg/hr for a natural gas feed of 1 kmol/hr. To find the optimum conditions, the costing for the system must also be introduced.

A range of temperatures and steam-to-carbon ratios of 860°C to 900°C and two to three, respectively, were evaluated to find the mass of hydrogen per production cost in US dollars. The data collected is shown in Figure 9 and the optimum point appears to be near 880°C with a steam-to-carbon ratio of two.

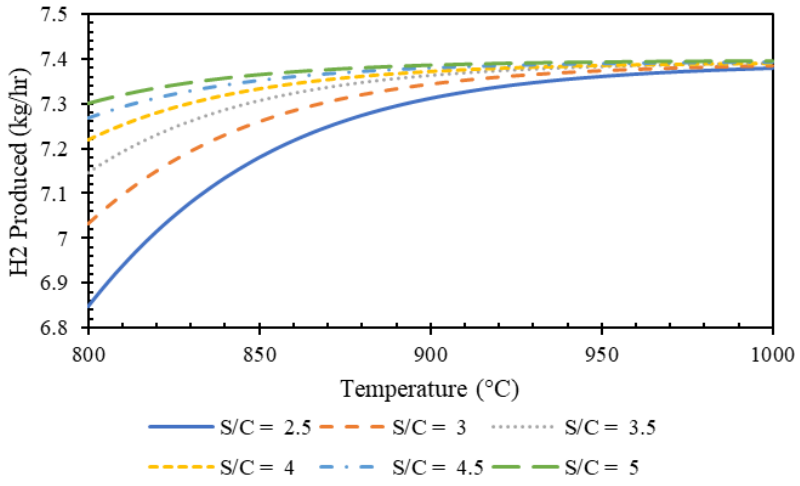

Figure 8. Hydrogen produced via SMR with varied temperature and S/C

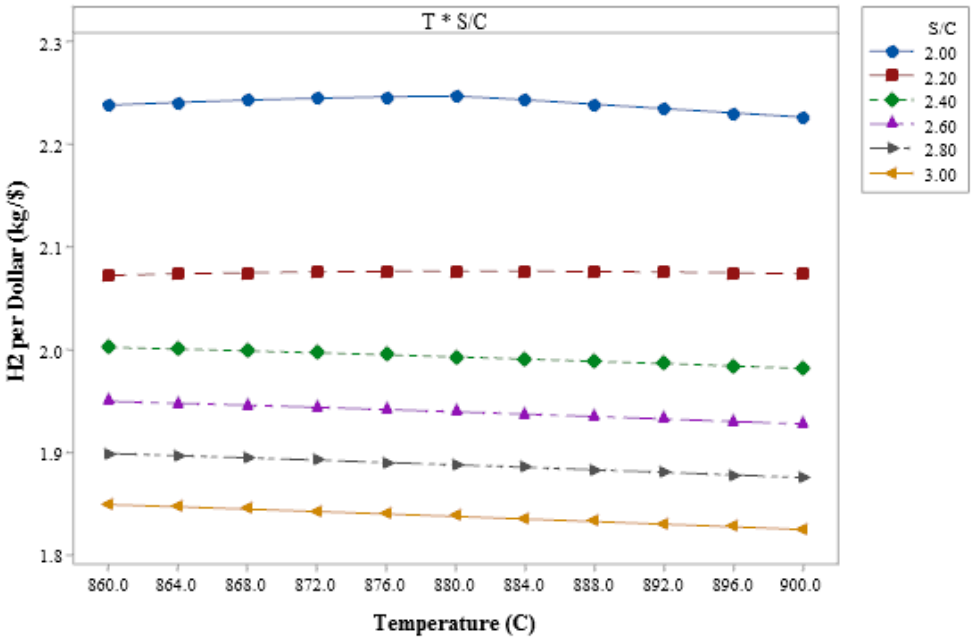

Figure 9. Hydrogen produced per US dollar with varied temperature and steam-to-carbon ratio for SMR

With this information, the domain of the searching variables was reduced and the PSO technique could be implemented successfully. The search area used for the PSO was a temperature range from 875 to 885°C and a steam-to-carbon range from 2 to 2.1. The PSO sub-procedure, shown in Appendix A, is used in conjuction with the Aspen Simulation Workbook. A custom table of relevant simulation variables was created in the Aspen Plus simulation and this table is shown in

Figure 10. Aspen Plus custom tables can be exported to Microsoft Excel and connected to the simulation with links. This allows the variable information to be sent between the simulation and the Excel spreadsheet using the table shown in Figure 11.

SMR

Name	Units	Value
NG Feed	kmol/hr	100
Water Feed	kmol/hr	202.839
NG P	bar	10
Steam P	bar	10
SMR T	C	882.481
NG Cost	$/sec	0.000258812
Water Cost	$/sec	0.00162812
Utility Cost	$/sec	0.0880547
SMR Q	Watt	6.75714e+06
H2 Out	kg/hr	719.609
CO2 Out	kg/hr	4192.27

Figure 10. Example of the Aspen Plus custom table

SMR				
Name	Units	Value	Low	High
NG Feed	kmol/hr	1		
Water Feed	kmol/hr	3	250	500
SMR T	C	900	800	1000
NG P	bar	10		
Steam P	bar	10		
NG Cost	$/sec	2.59E-06		
Water Cost	$/sec	2.41E-05		
Utility Cost	$/sec	1.09E-03		
SMR Q	Watt	7.02E+04		
H2 Out	kg/hr	7.34		
CO2 Out	kg/hr	42.80		
H2	kg/$	1.83		

Figure 11. Example of the Aspen Plus custom table in Microsoft Excel

To use the PSO sub-procedure, information about the system must be specified. This information includes the objective function, variables, and minimum and maximum

constraints on the variables. For this specific experiment, the objective function is the mass of hydrogen produced per dollar and is used in cell E17 of the table shown in Figure 11. Equation (9) is used to calculate the kilogram of hydrogen produced per US dollar,

$$\frac{H_2}{\$} = \frac{\dot{m}_{H_2}}{C_{NG} + C_W + C_U} \tag{9}$$

where C_{NG} is the cost of natural gas ($/hr), C_W is the cost of water ($/hr), and C_U is the cost of utilities ($/hr).

The optimization was conducted to maximize the amount of hydrogen produced per dollar of production cost, rather than minimizing the cost per hydrogen produced. The former allows for the optimization to converge and the inverse of the result is the production cost per unit hydrogen. If the latter were implemented, the result of the optimization would be zero: the best scenario for minimizing the cost is to not produce anything at all. The resulting value for the kilograms of hydrogen produced per production cost can simply be reciprocated to obtain the more appropriate result, production costs per kilogram of hydrogen produced.

The PSO sub-procedure converged on the optimum conditions of 882°C, with a steam-to-carbon ratio of 2.03, resulting in 2.22 kg H_2/$, or $0.45/kg H_2. This production cost matches quite well with the literature value of $0.47/kg H_2, calculated by Equation (5). [13] This temperature is within the realm of expected values given in literature. [4], [18] The S/C value is also realistic as the stoichiometric relation of methane and water for the reaction, shown in Equation (8) is two water to one methane. However, the S/C could be expected to be larger due to the WGS reaction. This reaction, shown in Equation (7), requires water

to react with carbon monoxide to produce more hydrogen. This could account for the 0.03 increase to the S/C, above the stoichiometric ratio.

The physical and chemical results of the solar SMR experiments were assumed to be the same as the results for the SMR experiments. However, as stated previously, the economic results are different due to the variation in utility costs. With these changes in the calculations, the optimum conditions for the solar SMR process were 882°C and S/C of 2.03, resulting in 6.69 kg H_2/$, or \$0.15/kg H_2.

Finally, an experiment was designed to test the SMC model. The process model was nearly identical to that of the previous two processes, however, the reaction section included only one reactor, as shown in Figure 12. This reactor is once again a Gibbs reactor to drive the model toward a more perfect result. Given literature values, the experiment was designed to vary temperature from 1227 to 2727°C, and evaluate the hydrogen produced at each temperature. [29] The results for this experiment are shown in Figure 13. The mass of hydrogen output begins to plateau near 2000°C, converging upon the reaction's equilibrium temperature.

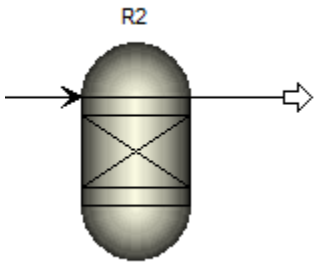

Figure 12. Reactor phase of SMC

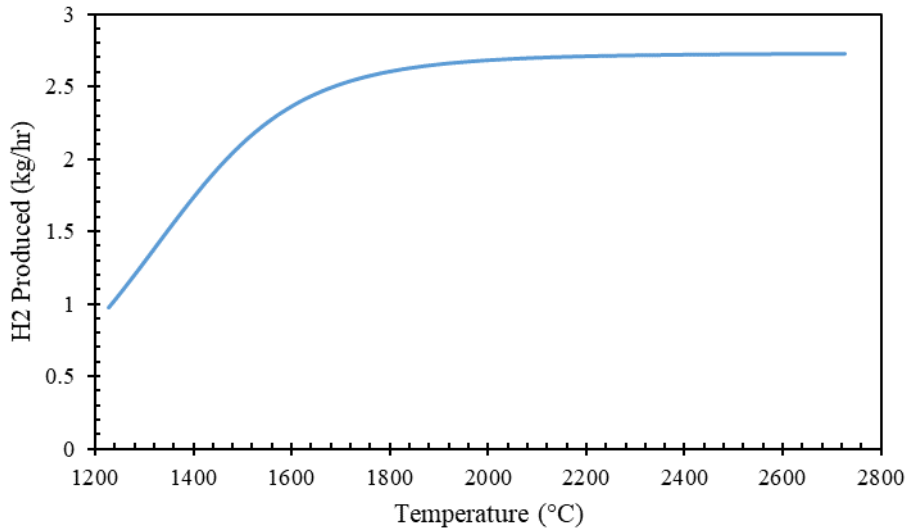

Figure 13. Hydrogen produced by the SMC model with varied temperature

To find the true optimum conditions of the process, the economic information must be introduced, once again. When including the cost of the natural gas feed and the utility cost of the model, the optimum temperature appears to be near 1900°C, as shown in Figure 14. This is the result of the ideal reaction temperature and the production cost competing against one another. If the objective were to increase hydrogen yield to the highest amount possible, the temperature would, of course, be increased to the highest amount possible, to ensure complete conversion of methane. However, the objective is to determine the optimum conditions to maximize the hydrogen yield while minimizing the production cost.

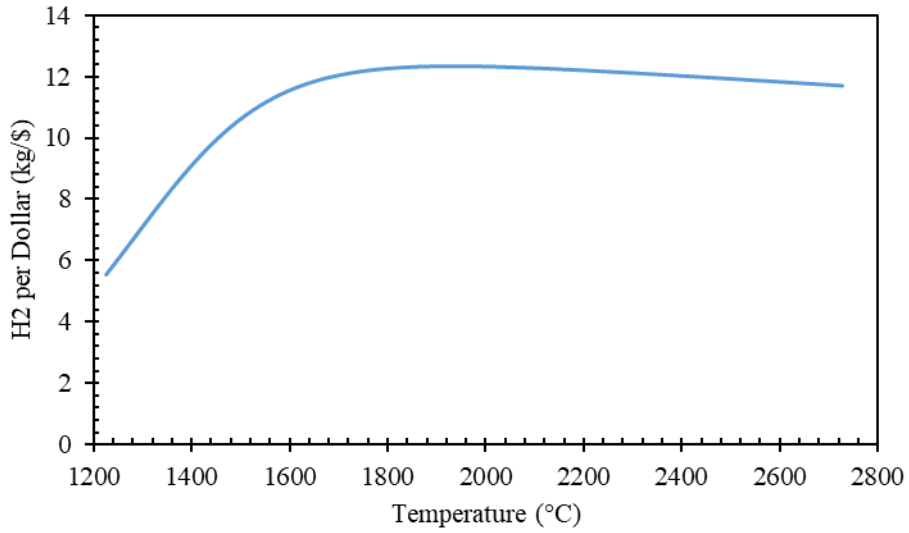

Figure 14. Hydrogen produced per US dollar via SMC

As before with the SMR optimization, this data allowed the search region to converge on a range from 1800 to 2000°C. For the SMC experiment, the PSO sub-procedure converged on the optimum temperature of 1942°C, resulting in 12.35 kg H_2/$, or \$0.08/kg H_2. The optimum conditions found for each of the three experimental procedures are shown in Table 3.

Table 3. Operating conditions and results for the production processes

Method	Temperature (°C)	Pressure (bar)	Steam-to-Carbon Ratio	Heat Duty (W)	H_2 Production Cost ($/kg)
SMR	882	10	2.03	7.02E+04	$ 0.45
Solar SMR	882	10	2.03	7.02E+04	$ 0.15
SMC	1942	10	-	9.25E+04	$ 0.08

The solar-powered process costs also include the costs for the heliostats as the main energy source for the reactions. This cost of heliostats per kilogram of hydrogen produced hourly was calculated using Equation (4) in Economic Analysis and the results for the solar SMR and the SMC processes are shown in Table 4. These results show that the solar SMR process requires a much lower cost of heliostats per production than the SMC process. This discrepancy is the result of the elevated heat duty for the SMC process as well as the different stoichiometry of the two processes. The increased heat duty for the SMC process is required to break the strong bonds between the carbon and hydrogens found in methane. Equation (8) in Process and Model Descriptions is the overall reaction for the SMR reactions and shows that the hydrogen production per methane consumption ratio is four. This ratio is double that of the SMC reaction, shown in Equation (8). This means that the SMR process is expected to produce roughly double the amount of hydrogen per unit methane versus the SMC process, while operating at a lower temperature. This results in a smaller amount of heliostats required to produce a larger amount of hydrogen.\

Table 4. Heliostat cost for the solar-powered processes.

Method	**Cost per H_2 hourly ($/kg/hr)**
Solar SMR	332.59
SMC	1,184.27

In addition to hydrogen production costs, carbon emissions is an important characteristic of each evaluated process. SMR is expected to result in the most carbon emissions, given both the CO_2 byproduct from the reactions as well as the energy source of the process: a high temperature, natural gas furnace. Both solar SMR and SMC have drastically reduced

carbon emissions in comparison to SMR, due to the solar-powered reactors. However, both processes do emit a small amount of CO_2 simply from the reactions used. Following the optimization of each process, the total carbon emissions were calculated with the data are shown in Table 5. As the results indicate, the SMR process produces drastically more carbon emissions than either of the solar-powered processes. This result was expected due to the natural gas furnace used to reach the reaction temperature. These carbon emission totals include any emissions related to the utilities of the processes.

Table 5. Carbon emissions per hydrogen produced.

Method	**CO_2e/H_2 (kg/kg)**
SMR	283
Solar SMR	0.61
SMC	0.57

As the results show, the conventional SMR method of hydrogen production has the highest production cost of the three processes. This is most likely the result of increased utility costs associated with heating the main reactor to such a high temperature as 882°C. This is evident when comparing the production cost to that of the solar SMR process. The $0.30/kg difference can only be explained by this cause, as these two processes are identical otherwise.

When comparing the production costs of the solar SMR and the SMC processes, there is a mere $0.07 discrepancy. This added cost for the solar SMR process comes from the additional operations required for the processes, such as the WGS reactors and the utilities

associated. This added cost seems inconsequential when taking into account the cost of heliostats for the two processes.

Given these results, it is recommended to pursue solar SMR for hydrogen production moving forward. Solar SMR provides a greater yield of hydrogen with reduced production costs. Although the process results in production costs slightly higher than those of SMC, solar SMR requires a lower reaction temperature, thus a lower heat duty for the main reaction, and a lower capital cost for heliostats as compared to SMC. Solar SMR also emits an insignificant amount of carbon dioxide per hydrogen produced in relation to the traditional SMR process. The variance between the carbon emissions for solar SMR and SMC is unimportant.

CONCLUSION

Three different hydrogen-producing processes were simulated and optimized. The processes in question were steam methane reforming (SMR), solar SMR, and solar methane cracking (SMC). Aspen Plus simulation software was used to simulate the processes and the optimizations were conducted via the statistical experimental factorial design method with Minitab and the PSO technique using integration between Microsoft Excel and Aspen Plus. The processes were optimized to produce the maximum mass of hydrogen per US dollar of production cost. Upon optimization, each process was analyzed to determine the appropriate process to implement in future projects. The main parameters in question are the hydrogen production cost, the solar energy collection cost, and the amount of carbon emissions.

After investigating the results, it is recommended to implement solar-powered reactors in the SMR process. The SMR reactions, coupled with water-gas shift reactions, produce an

increased yield of hydrogen per production cost, while simultaneously reducing the carbon emissions of the process. Implementation of SMC is not recommended at this time, as the cost of the heliostats required is substantially more than that of the solar SMR process.

Following this research, there are recommendations for future work. It is recommended that the simulations incorporate more accurate reactor models based on the reaction kinetics. This work follows the conditions and schemes of experimental systems found in literature. However, an even more accurate model could be created by integrating particle flow or dynamic heating in the reactors. This could allow for a better understanding of the sensitivity of the solar-powered processes with respect to the solar energy provided to the reactor. Also, the economic analysis of these processes should be further investigated. Aspen Plus has the capabilities to calculate capital costs and report the feasibility and ease of investment of models. These tools can be used to increase the accuracy of the production costs throughout the years and into the future.

REFERENCES

[1] B. Parkinson *et al.*, “Hydrogen production using methane: Techno-economics of decarbonizing fuels and chemicals,” *Int J Hydrogen Energy*, 2018.

[2] S. Touili, A. Alami Merrouni, A. Azouzoute, Y. El Hassouani, and A. Amrani, “A technical and economical assessment of hydrogen production potential from solar energy in Morocco,” 2018.

[3] T. Pregger, D. Graf, W. Krewitt, C. Sattler, M. Roeb, and S. Möller, “Prospects of solar thermal hydrogen production processes,” 2009.

[4] A. Pareek, R. Dom, J. Gupta, J. Chandran, V. Adepu, and P. H. Borse, “Insights into renewable hydrogen energy: Recent advances and prospects.”

[5] “Aspen Plus | Leading Process Simulation Software | AspenTech.” [Online]. Available: https://www.aspentech.com/en/products/engineering/aspen-plus. [Accessed: 11-Jun-2020].

[6] “Data Analysis, Statistical & Process Improvement Tools | Minitab.” [Online]. Available: http://www.minitab.com/en-US/default.aspx. [Accessed: 11-Jun-2020].

[7] “Microsoft Excel, Spreadsheet Software, Excel Free Trial.” [Online]. Available: https://www.microsoft.com/en-us/microsoft-365/excel. [Accessed: 11-Jun-2020].

[8] R. A. Davis, *Practical Numerical Methods for Chemical Engineers: Using Excel with VBA*, 4th ed. Duluth, MN, 2018.

[9] R. Hassan, B. Cohanim, O. De Weck, and G. Venter, “A comparison of particle swarm optimization and the genetic algorithm,” in *Collection of Technical Papers - AIAA/ASME/ASCE/AHS/ASC Structures, Structural Dynamics and Materials Conference*, 2005.

[10] M. Sengupta, Y. Xie, A. Lopez, A. Habte, G. Maclaurin, and J. Shelby, “The National Solar Radiation Data Base (NSRDB),” *Renewable and Sustainable Energy Reviews*, vol. 89. Elsevier Ltd, pp. 51–60, 01-Jun-2018.

[11] “Water and Wastewater Annual Price Escalation Rates for Selected Cities across the United States,” 2017.

[12] “Natural Gas Industrial Price.” [Online]. Available: https://www.eia.gov/dnav/ng/ng_pri_sum_a_EPG0_PIN_DMcf_a.htm. [Accessed: 26-Mar-2020].

[13] A. M. Amin, E. Croiset, and W. Epling, “Review of methane catalytic cracking for hydrogen production,” 2010.

[14] “Heat Content of Natural Gas Delivered to Consumers.” [Online]. Available: https://www.eia.gov/dnav/ng/ng_cons_heat_a_EPG0_VGTH_btucf_a.htm. [Accessed: 22-Apr-2020].

[15] S. Möller, D. Kaucic, and C. Sattler, “Hydrogen production by solar reforming of natural gas: A comparison study of two possible process configurations,” *J Sol*

Energy Eng Trans ASME, vol. 128, no. 1, pp. 16–23, Feb. 2006.

[16] "XE: Convert EUR/USD. Euro Member Countries to United States Dollar." [Online]. Available: https://www.xe.com/currencyconverter/convert/?Amount=1&From=EUR&To=USD. [Accessed: 11-Jun-2020].

[17] D. Graf, N. Monnerie, M. Roeb, M. Schmitz, and C. Sattler, "Economic comparison of solar hydrogen generation by means of thermochemical cycles and electrolysis," 2008.

[18] J. C. Molburg and R. D. Doctor, "Hydrogen from Steam-Methane Reforming with CO 2 Capture."

[19] "Chemical Composition of Natural Gas - Union Gas." [Online]. Available: https://www.uniongas.com/about-us/about-natural-gas/chemical-composition-of-natural-gas. [Accessed: 12-Mar-2020].

[20] W. Stein, J. Edwards, J. Hinkley, and C. Sattler, "Natural Gas: Solar-Thermal Steam Reforming," *Encycl Electrochem power sources*, pp. 300–312, 2009.

[21] G. J. Kolb *et al.*, "SANDIA REPORT Heliostat Cost Reduction Study," 2007.

[22] C. Chen, M. H. Back, and R. A. Back, "Dissociation of Methane and its Pressure Dependence1-2."

[23] O. Olsvik, O. A. Rokstad, and A. Holmen, "Pyrolysis of methane in the presence of hydrogen," *Chem Eng Technol*, vol. 18, no. 5, pp. 349–358, Oct. 1995.

[24] S. Abanades and G. Flamant, "Experimental study and modeling of a high-temperature solar chemical reactor for hydrogen production from methane cracking," *Int J Hydrogen Energy*, vol. 32, pp. 1508–1515, 2007.

[25] D. Hirsch, M. Epstein, and A. Steinfeld, "The solar thermal decarbonization of natural gas," 2001.

[26] G. Maag, S. Rodat, G. Flamant, and A. Steinfeld, "Heat transfer model and scale-up of an entrained-flow solar reactor for the thermal decomposition of methane," 2010.

[27] S. Rodat, S. Abanades, and G. Flamant, "Co-production of hydrogen and carbon black from solar thermal methane splitting in a tubular reactor prototype," 2010.

[28] C. Hu, S. Zhang, and H. Li, "Methane pyrolysis in preparation of pyrolytic carbon: Thermodynamic and kinetic analysis by density functional theory."

[29] B. Nezzari and R. Gomri, "Study of cracking of methane for hydrogen production using concentrated solar energy," 2019.

APPENDIX A: VBA CODE

Listed below are the Visual Basic sub-procedures used for the optimization.

```
Public Sub AspenLink()
'Runs the Aspen Simulation Workbook with current parameters and waits
        Call ASWRunActiveSimulation
        Call WaitTime(3)
        Call WaitTime(0.5)
End Sub

Public Sub WaitTime(t)
'Procedure to force Excel to wait t seconds before continuing
        newHour = Hour(Now())
        newMinute = Minute(Now())
        newSecond = Second(Now()) + t
        WT = TimeSerial(newHour, newMinute, newSecond)
        Application.Wait WT
End Sub

Public Sub PSO()
‘Adapted from [8]
' Davis modifications to Particle Swarm Optimization method for minimization of a multimodal objective function. Uses Latin Hypercube particle initialization of the variable domain. An adaptive inertia factor uses particle success feedback
' (Nickabadi,et al. (2011) App. Soft Computing J., vol. 11,  no. 4, pp. 3658-3670).
' Requires the function in a worksheet cell in terms of a range of variables on the worksheet.  Also requires corresponding ranges for the variable lower and upper bounds.  The user may specify inertia and acceleration factors: w, c1, c2.

' *** Required Worksheet Setup ***
' Input1: fr = Cell with the formula for the objective function, f(x)
' Input2: xr = Range of variables of optimization, x
' Input3: xlr = Range of variables lower bounds
' Input4: xur = Range of variables upper bounds
' Input5: imax = Maximum cycles
```

```
' Input6: cmax = Maximum cycles with no change in x
' Input7: m = Particle population size
' Input8: w = Inertia weight
' Input9: c1 = Local acceleration factor
' Input10: c2 = Global acceleration factor
' Output1 = Location of minimum and f are final values in ranges for x and f

' *** Required VBA procedures from PNMSuite ***
' RNDWH = function for random number generation (Ch03_VBA)

' *** Nomenclature ***
Const bxtl As String = "PSODM" ' = input box title
Const small As Double = 0.00000001 ' = small number to avoid division by zero
Dim c As Long ' = convergence counter index to check for change between cycles
Dim cmax As Long ' = maximum cycles without change for convergence
Dim c1 As Double, c2 As Double ' = acceleration constants (typically 1.5 to 2)
Dim dj() As Double ' = dx for Latin hypercube sampling
Dim dx() As Double ' = size of domain of variable between lower and upper limits
Dim dxl As Double, dxu As Double ' = lower and upper distance to boundaries
Dim f() As Double, fg As Double ' = particle function values and best function value
Dim fr As Range ' = range address of the objective function
Dim g As Long ' = fittest particle index
Dim j As Long, k As Long ' = index for variables (j) and particles (k)
Dim i As Long, imax As Long ' = cycles and maximum cycles for PSO
Dim m As Long ' = number of particles (each with dimension n)
Dim n As Long ' = number of variables
Dim p() As Double ' = individual particle best position
Dim s As Double, ps As Double ' = success sum and particle success factor
Dim t As Double ' temporary value for shuffling initial coordinates
Dim v() As Double ' = particle "velocity" vector
Dim w As Double ' = inertia weight factor (typically 0.5)
Dim x() As Double ' = array of particle coordinates (optimization variables)
Dim xg() As Double ' = global best particle coordinates
```

```
Dim xr As Range ' = range address of variables on the worksheet
Dim xlr As Range, xur As Range ' = range of lower and upper bounds on variables
Dim xl() As Double, xu() As Double ' = lower and upper limits on variables
'**********************************************************************
On Error Resume Next ' catch input cancel errors

With Application
.Calculation = xlCalculationAutomatic ' turn on worksheet automatic calculation

Set fr = .InputBox(prompt:="Cell of Objective FUNCTION, f(x):", Title:=bxtl, Type:=8)
   If Err.Number = 424 Then Exit Sub
Set xr = .InputBox(prompt:="Range of VARIABLE(S), x:", Title:=bxtl, Type:=8)
   If Err.Number = 424 Then Exit Sub
n = xr.Count ' number of variables of optimization
Set xlr = .InputBox(prompt:="Range of Variable LOWER Bounds:", Title:=bxtl, Type:=8)
   If Err.Number = 424 Then Exit Sub
Set xur = .InputBox(prompt:="Range of Variable UPPER Bounds:", Title:=bxtl, Type:=8)
   If Err.Number = 424 Then Exit Sub
If n <> xlr.Count Or n <> xur.Count Then ' check for consistency of variable settings
   MsgBox "Number of variables must match the number of lower/upper bounds."
   Exit Sub
End If
imax = .InputBox(prompt:="Maximum CYCLES:", Title:=bxtl, default:=1000, Type:=1)
   If Err.Number = 424 Then Exit Sub
   imax = .Max(CInt(imax), 10)
cmax = .InputBox(prompt:="Maximum Cycles with NO CHANGE:", Title:=bxtl, default:=20 * n,
Type:=1)
   If Err.Number = 424 Then Exit Sub
   cmax = .Max(CInt(cmax), 2)
m = .InputBox(prompt:="Particle POPULATION Size:", Title:=bxtl,
default:=.Min(15 * n, 50), Type:=1)
   If Err.Number = 424 Then Exit Sub
   m = .Max(CInt(m), 10)
w = .InputBox(prompt:="Inertia WEIGHT:", Title:=bxtl, default:=0.5, Type:=1)
```

```
   If Err.Number = 424 Then Exit Sub
c1 = .InputBox(prompt:="Local Particle ACCELERATION Factor:", Title:=bxtl, default:=1.5, Type:=1)
   If Err.Number = 424 Then Exit Sub
c2 = .InputBox(prompt:="Global Particle ACCELERATION Factor:", Title:=bxtl, default:=1.5, Type:=1)
   If Err.Number = 424 Then Exit Sub

.ScreenUpdating = False ' to speed up the calculations, turn of auto-screen-updating

ReDim dj(1 To n) As Double, f(1 To m) As Double, p(1 To m, 1 To n) As Double, v(1 To m, 1 To n) As
Double, x(1 To m, 1 To n) As Double, dx(1 To n) As Double, xg(1 To n) As Double, xl(1 To n) As Double,
xu(1 To n) As Double

For j = 1 To n ' check for relative lower and upper limits on variables
   xu(j) = .Max(xur(j), xlr(j)): xl(j) = .Min(xur(j), xlr(j))
   dx(j) = xu(j) - xl(j): dj(j) = dx(j) / m
Next j

For j = 1 To n ' Check for initial variable consistency with limits and first particle
   If xr(j) < xl(j) Or xr(j) > xu(j) Then xr(j) = xl(j) + RNDWH() * dx(j)
Next j

For k = 1 To m ' Use Latin Hypercube Sampling to initialize particles
   For j = 1 To n: x(k, j) = xl(j) + (k - 1 + RNDWH()) * dj(j): Next j
Next k

For j = 1 To n ' Random shuffle of variables for initial particles
   For k = m To 1 Step -1
      i = Int(k * RNDWH + 1): t = x(i, j): x(i, j) = x(k, j): x(k, j) = t
   Next k
Next j

For k = 1 To m ' Initialize the population of particles and velocities
   For j = 1 To n ' variable initialization loop
      p(k, j) = x(k, j): xr(j) = p(k, j): v(k, j) = 0 ' initial particle & velocity
```

```
   Next j
   f(k) = fr
   If Not k = 1 Then
      If f(k) > fg Then ' record the global best particle function and index          *** BR Edit "f(k) > fg" from "f(k) < fg"
         fg = f(k): g = k
         For j = 1 To n: xg(j) = x(g, j): Next j
      End If
   Else
      fg = f(k): g = 1 ' use the first particle as the initial global best
   End If
Next k

c = 0: ps = 1 ' initialize counter for checking convergence & particle success factor
For i = 1 To imax ' overall search PSO loop
   c = c + 1 ' search convergence counter
   s = 0 ' reset the success factor
   For k = 1 To m ' particle loop
      For j = 1 To n ' variable loop
         v(k, j) = ps * w * v(k, j) _
               + RNDWH() * c1 * (p(k, j) - x(k, j)) _
               + RNDWH() * c2 * (p(g, j) - x(k, j)) ' velocity
         dxl = Abs(x(k, j) - xl(j)): dxu = Abs(x(k, j) - xu(j)) ' distance to bound
         x(k, j) = x(k, j) + v(k, j) ' new x
         If x(k, j) < xl(j) Then ' prevent x from exceeding limits
            x(k, j) = xl(j) + dxl * Abs((x(k, j) - xl(j)) / v(k, j))
         ElseIf x(k, j) > xu(j) Then
            x(k, j) = xu(j) - dxu * Abs((x(k, j) - xu(j)) / v(k, j))
         End If
         xr(j) = x(k, j) ' set the variables on the worksheet to calculate f
      Next j
      If fr > f(k) Then ' update particle best coordinates and fitness value          *** BR Edit "fr > f(k)" from "fr < f(k)"
         f(k) = fr: s = s + 1 ' upgrade the best particle function value
```

```
            For j = 1 To n: p(k, j) = x(k, j): Next j ' save local best particles
            If f(k) > fg Then ' new global best particle '                    *** BR Edit "f(k) > fg" from "f(k) < fg"
               c = 0: fg = f(k): g = k ' reset counter & save global best part. index
            End If
         End If

         Call AspenLink '                                                    *** BR Edit

      Next k

      If Not c = cmax Then ' check for reaching convergence cycle limit
         ps = s / m ' normalize particle success factor
         If i Mod 10 = 0 Then .StatusBar = bxtl & " Cycle: " & i _
                  & ", Converged: " & VBA.Format(c / cmax, "0%") _
                  & ": OF = " & VBA.Format(fg, "#.###E+##")
      Else
          Exit For
      End If
   Next i
   .StatusBar = bxtl & " Cycle: " & i & ", Converged: " & VBA.Format(c / cmax, "0%")
   For j = 1 To n: xr(j) = p(g, j): Next j ' report the best particle coordinates

   fr.Select ' Add comment to function cell
   With ActiveCell
      .ClearComments: .addcomment
      With .comment
         .Visible = False
         .Text Text:="PNMSuite: " & bxtl & vbNewLine _
            & "Objective Function f(x) = " & fr.Address & vbNewLine _
            & "Variable Range = " & xr.Address & vbNewLine _
            & "Lower Bounds = " & xlr.Address & vbNewLine _
            & "Upper Bounds = " & xur.Address & vbNewLine _
            & "Maximum Cycles = " & imax & vbNewLine _
```

```
            & "Maximum Convergence Cycles = " & cmax & vbNewLine _
            & "Population Size = " & m & vbNewLine _
            & "Inertia Weight Factor = " & w & vbNewLine _
            & "Particle Acceleration Factor = " & c1 & vbNewLine _
            & "Global Acceleration Factor = " & c2 & vbNewLine _
            & VBA.Date & " at " & VBA.Time
        .Shape.TextFrame.AutoSize = True
    End With ' Comment
End With ' ActiveCell

.ScreenUpdating = True: beep
End With ' Application
End Sub ' PSO

Public Static Function RNDWH() As Double
‘Adapted from [8]
'*************************************************************************
' Wichmann-Hill Pseudo Random Number Generator (PRNG) with a period of ~ 10^36. The
' PRNG is initialized by the Timer, or internal computer clock. This is an alternative
' for VBA Rnd() function (period is ~10^6). Note: the static function is required to
' preserve the values of the constants between calls to the function.

' *** Nomenclature ***
Dim f As Boolean ' = flag to check for initialization
Dim r As Double ' = random number
Dim s As Double ' = initialization seed for the PRNG
Dim t As Long, x As Long, y As Long, z As Long ' = integer values for PRNG algorithm
'*************************************************************************
On Error Resume Next ' Skip over random errors

' Note that True conditions run faster in VBA. t, x, y & z must be > 0.
' Mod divides two numbers and returns only the remainder
If f = True Then ' Congruential algorithm
```

```
    x = 11600 * (x Mod 185127) - 10379 * (x / 185127)
    y = 47003 * (y Mod 45688) - 10479 * (y / 45688)
    z = 23000 * (z Mod 93368) - 19423 * (z / 93368)
    t = 33000 * (t Mod 65075) - 8123 * (t / 65075)
Else ' Initialize pseudo-random-number-generator (PRNG). Use the computer clock to
     ' generate seed for PRNG. Timer returns number of seconds elapsed since 12 am.
    s = Timer * 60#
    x = 11600 * (s Mod 185127) - 10379 * (x / 185127)
    y = 47003 * (s Mod 45688) - 10479 * (y / 45688)
    z = 23000 * (s Mod 93368) - 19423 * (z / 93368)
    t = 33000 * (s Mod 65075) - 8123 * (t / 65075)
    f = True
End If

If x > 0 Then Else x = x + 2147483579 ' Use fast x > 0 Then 'do nothing' Else
If y > 0 Then Else y = y + 2147483543
If z > 0 Then Else z = z + 2147483423
If t > 0 Then Else t = t + 2147483123

' Random number, CDbl returns a double precision value
r = CDbl(x) / 2147483579 + CDbl(y) / 2147483543 _
  + CDbl(z) / 2147483423 + CDbl(t) / 2147483123

RNDWH = r - Int(r) ' Uniform random deviate (0<r<1)

End Function ' RNDWH
```